

LAS-TR-E165-7

APR 26 1961

MARCH 1961

SN-84820

FINAL

HS-53

NASA CR 51854
N 68 85258
Order 5

**MEASUREMENT OF COMPOSITION AND ENERGY SPECTRUM
OF PRIMARY COSMIC RADIATION**

James E. Lamport

Final

Technical Progress Report



THE UNIVERSITY OF CHICAGO

LABORATORIES FOR APPLIED SCIENCES

NASA CR - 51854

LAS-TR-E165-7

MARCH 1961

33 p 0 ref

↑
**MEASUREMENT OF COMPOSITION AND ENERGY SPECTRUM
OF PRIMARY COSMIC RADIATION**

James E. Lamport

Final

Technical Progress Report

(NASA Contract No. NASw-24)

SN - 84820 [index]

University Research Division
National Aeronautics and Space Administration
Washington, D.C.

1884006

2/ LABORATORIES FOR APPLIED SCIENCES
S. 6220 South Drexel Avenue
Chicago 37, Illinois
U.I.

FOREWORD

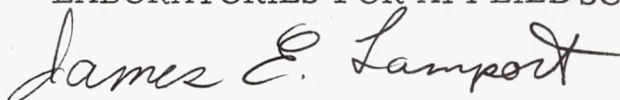
This is the final progress report under National Aeronautics and Space Administration (NASA) Contract No. NASw-24 entitled, "Measurement of Composition and Energy Spectrum of Primary Cosmic Radiation." Work under this contract was initiated during May 1959.

The breadth of the work statement contained in Contract NASw-24 has allowed a series of developments which would not otherwise have been possible, thus providing for the University and NASA a highly profitable working arrangement. The cooperation and support of NASA personnel is greatly appreciated.

The preliminary equipment developed under this contract was flight-tested under Contract No. AF 29(600)-1759 with the Aeromedical Field Laboratory of Holloman Air Force Base.

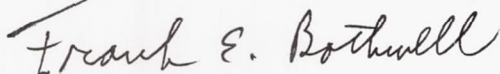
The University of Chicago personnel who have participated in this program include: B. E. Arneson, L. Bess, L. M. Biberman, C. M. Cohn, C. Y. Fan, G. Gloeckler, W. P. Harvey, E. L. Hubbard, J. E. Lamport, P. Meyer, R. M. Natkin, M. A. Perkins, L. J. Petraitis, D. L. Sachs, J. A. Simpson, R. M. Takaki, A. J. Tuzzolino, W. A. Van Zeeland, and G. C. Wang.

LABORATORIES FOR APPLIED SCIENCES



James E. Lamport
Assistant Director

Approved:



Frank E. Bothwell
Director

TABLE OF CONTENTS

<u>Section</u>	<u>Page</u>
1. Introduction	1
2. Detection Techniques	1
2.1 Laboratory Instrumentation for Calibration of Detector Materials	3
2.2 Low-Energy Detector System	6
2.3 High-Energy Detector System	6
2.4 Gold-Silicon Detectors	9
3. Data Handling	14
3.1 Pulse-Height Analysis	14
3.2 Data Rate	21
3.3 Analysis and Grouping of Cosmic Ray Particles	21
3.3.1 Detection Range for Low-Energy Detector	21
3.3.2 Detection Range for High-Energy Detector	25
4. Flight Tests	26
5. Summary	26

LIST OF ILLUSTRATIONS

<u>Figure</u>	<u>Page</u>
1. The 200-Channel Pulse Height Analyzer Installation	4
2. Test Setup to Obtain the Energy Resolution Characteristics of Scintillator Crystals and Cerenkov Radiator Materials	5
3. Cross-Sectional View of Low-Energy Detection System	7
4. Cross-Sectional View of High-Energy Detection System	8
5. Resultant Type Approval Unit for Able-5 Instrumentation	11
6. Instrument Configuration	12
7. Energy Resolution for Gold-Silicon Solid State Detector	13
8. Block Diagram of System for the Monitoring of Low-Energy Cosmic Ray Primaries.	15
9. Preamplifier and Range Switch Assembly.	16
10. Programmer Board	19
11. Height-to-Time Converter Board	20
12. Shift Register and Readout Board	22

LIST OF TABLES

<u>Table</u>	<u>Page</u>
1. Range in Phenyl-Cyclohexane (gm/cm^2)	23
2. Rate of Energy Loss in Matter Referred to Phenyl-Cyclo- hexane	24
3. Assignment of Values for Events from Data of the Balloon Flight Test on 19 August 1959	27

1. INTRODUCTION

The primary cosmic-ray particles consist of protons, alpha particles, and nuclei of higher atomic number. Much information is needed about the charge and energy of these particles. The equipment required to obtain this information must be carried by some vehicle to high altitudes to remove the effects of the earth's atmosphere and magnetic field. It must (1) detect and classify the particles, and (2) preprocess, store, and transmit the data to the ground. The objective of this project has been to design and construct such equipment for particles whose energies lie in the range between 10's of Mev per nucleon and about 300 or 400 Mev per nucleon. When this program was started much of the theoretical and experimental information was already available from balloon-borne experiments performed earlier at the Enrico Fermi Institute for Nuclear Studies. With this experience as a basis, a program was begun to improve detection techniques, to develop pulse-height analysis circuitry suitable for use in satellites, and to study the techniques for on-board computation and storage of the information generated by the pulse-height analysis circuitry.

Systems using CsI scintillators and Cerenkov radiators and pulse-height analysis circuitry were developed to detect and classify both low and high-energy particles. This equipment was flown on balloons in cooperation with the Aeromedical Field Laboratory of Holloman Air Force Base. The results of these tests are presented herein.

A prototype instrument in which gold-coated silicon semiconducting wafers are used to measure the low-energy proton flux was developed and produced for use in the Atlas-Able-5 vehicle, which failed at launch. Similar equipment of a more complex design has been prepared under another contract for the Ranger I and II vehicles.

2. DETECTION TECHNIQUES

The investigation of detection techniques was divided. The primary effort was directed toward designing detection devices using CsI scintillators and Cerenkov detectors. The secondary effort was an investigation of semiconductor devices which might be used as direct detectors.

A cosmic-ray particle is approximately characterized by its charge or mass number and its kinetic energy. These quantities are implicit in the rate

of energy loss in matter. The kinetic energy is a measure of mass and velocity. Both energy loss rate and total kinetic energy may be measured by a system employing a pair of scintillators, one designed to present a density small enough to permit passage of the particle through its volume and the other designed to present sufficient density to bring the particle to rest. For particles whose energy is above about 500 Mev per nucleon, a measure of the kinetic energy may be obtained from the quantity of Cerenkov radiation emitted in an optically clear material of suitable refractive index ($n \geq 1.5$). Therefore, both the energy and charge or approximate mass can be determined by the solution of the simultaneous equations:

$$-\frac{dE}{dx}\bigg|_{\text{ion}} = \frac{4\pi Z^2 e^4 \eta}{V_m^2} \left(\ln \frac{2V_m^2}{\bar{I}(1-\beta^2)} - \beta^2 \right) \quad (1)$$

$$E = 1/2 M_0 V^2 \quad \text{over the range} \quad M_0 \simeq 2Z \quad (2)$$

$$\frac{dN}{dL} = \frac{4\pi^2 Z^2 e^2}{h c^2} \left(1 - \frac{1}{n^2 \beta^2} \right) d\gamma, \quad (3)$$

in which

Z = charge on the incoming particle

e = charge of the electron

V = particle velocity

m = electron mass

M_0 = rest mass of the incoming nucleus

η = number of electrons/cm³ in the absorber

\bar{I} = average ionization potential of the absorber in ergs

$\frac{dN}{dL}$ = the number of photons emitted per unit path length

$d\gamma$ = the light frequency range

n = refractive index of the Cerenkov radiator

h = Planck Constant

c = velocity of light.

β = ratio of particle velocity to velocity of light.

Simultaneous solution of Eqs. (1) and (2) above applies to those particles which are stopped within the scintillator telescope, i. e., nuclei having less than 500 Mev per nucleon.

Simultaneous solution of Eqs. (1) and (3) applies to relativistic particles.

The quantities which must be measured, then, are the energy and the energy loss rate. It is possible to obtain these quantities by the combinations of scintillation counters, Cerenkov radiators, and/or semiconductor (AuSi) detectors.

The use of scintillating materials such as CsI and NaI coupled to photomultiplier tubes is a proven technique for nuclear pulse-height analysis. The use of the materials has been extended to balloon flight applications in which pulse-height data have been registered photographically or transmitted directly in binary form.

2.1 LABORATORY INSTRUMENTATION FOR CALIBRATION OF DETECTOR MATERIALS

The detector characteristics for the cosmic-ray monitoring equipment were evaluated experimentally by using the 200-channel pulse-height analyzer shown in Fig. 1 which was purchased under Contract No. NASw-24. With this unit, it is possible to obtain the energy resolution characteristics of the scintillator crystals, Cerenkov radiator materials, and the AuSi detector. In measurements involving scintillators and Cerenkov radiators, the hard component of cosmic radiation used to calibrate the detectors is separated from the soft component by forcing the radiation to pass through a 5-cm thick lead brick, as shown in Fig. 2. A pair of plastic scintillators in a coincidence arrangement define the acceptance angle for the detector crystal under test. The output of this twofold coincidence telescope, in the form of a shaped gating pulse, is applied to the prompt coincidence input to insure that only those particles passing completely through the telescope are analyzed. The count rate obtainable under these conditions is approximately one per 3 to 6 minutes. A test run requires from 40 to 100 hours of continuous data collection to ensure sufficient statistical reliability.

To date, the calibration of the AuSi detector has been through use of particle emitters such as Cm^{242} , Cm^{244} , and Po^{210} . Two procedures have been used, the first to determine the energy resolution of the detector (Fig. 2) and the second to determine the detection threshold for the system including

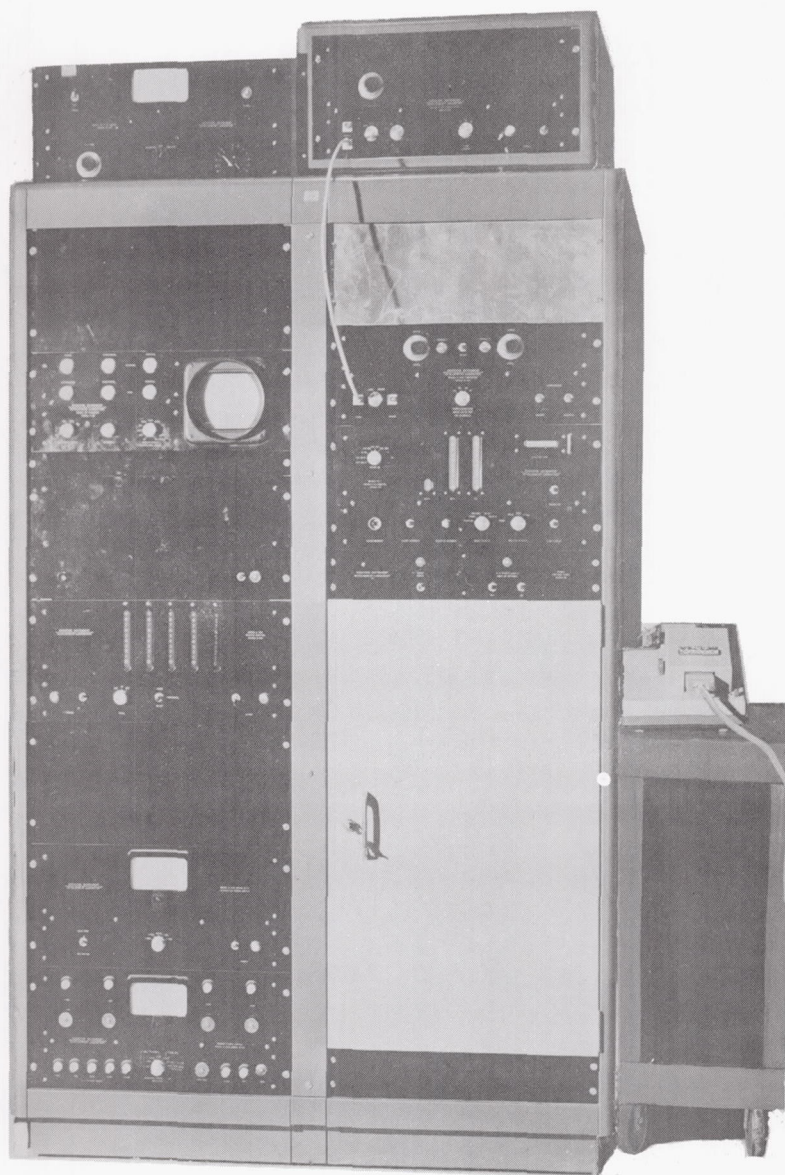


Figure 1. The 200-Channel Pulse Height Analyzer Installation

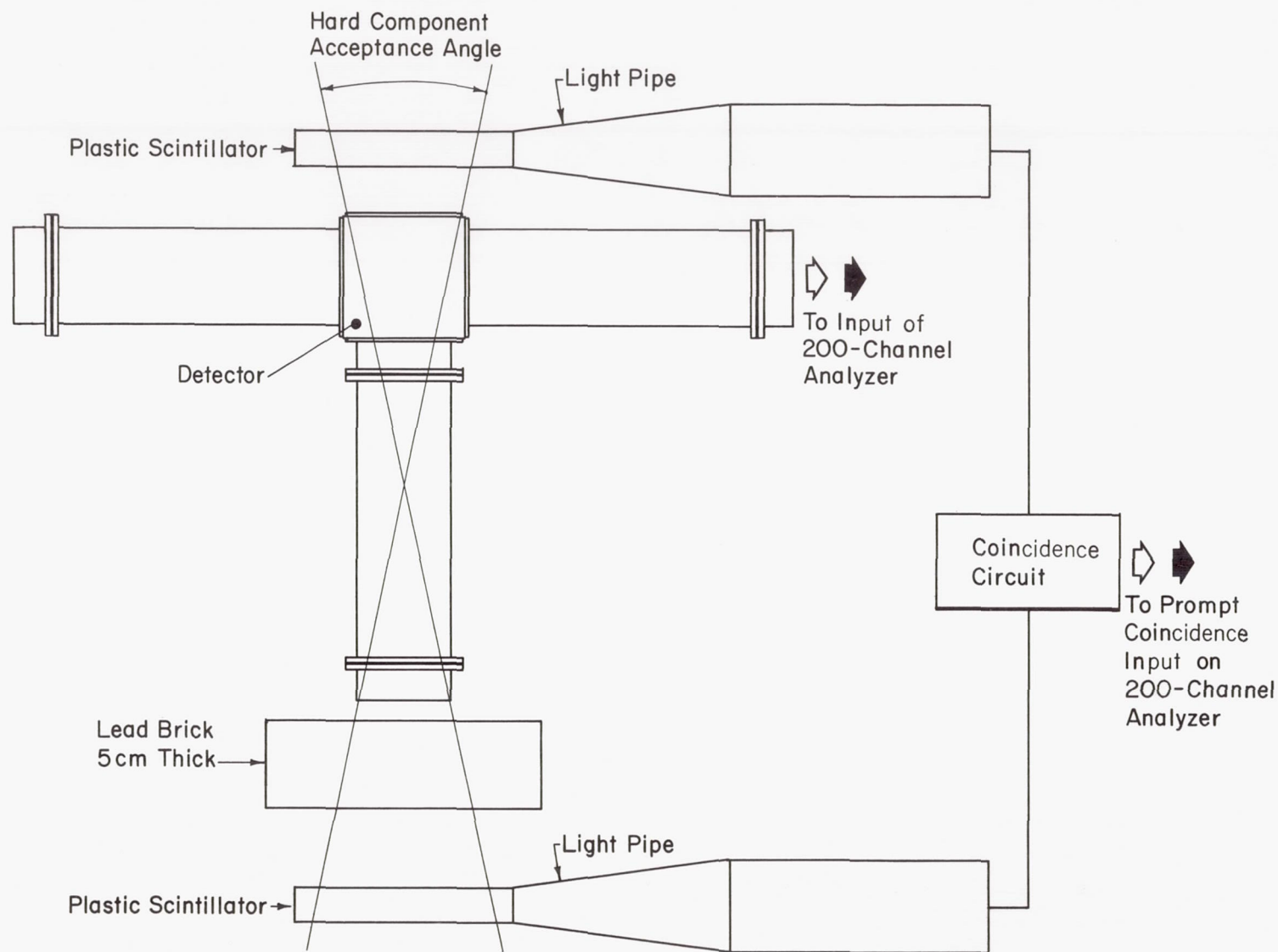


Figure 2. Test Setup to Obtain the Energy Resolution Characteristics of Scintillator Crystals and Cerenkov Radiator Materials

detector, amplifier, and discriminator. The latter determination is a function of the combination of detector and electronic characteristics. At the present time the energy threshold is limited by the noise inherent in the transistorized electronic circuit design.

2.2 LOW-ENERGY DETECTOR SYSTEM

Figure 3 is a cross-sectional view of a system to detect particles of energy between 50 and 500 Mev/nucleon. The unit consists of three scintillator elements and their associated photomultiplier tubes. In this system incident particles first pass through the 1/32 in. thick thallium-activated cesium-iodide scintillator (detector 1). This scintillator measures the rate of energy loss.

The 3-cm thick cesium-iodide scintillator (detector 2) measures total energy. The light pulses from the two cesium-iodide scintillators are viewed by their respective photomultiplier tubes whose outputs are applied to the pulse-height analysis systems discussed in section 3.

The plastic scintillator (detector 3) surrounds the large cesium-iodide crystal and is in anticoincidence with the other two detectors. Thus, those particles below the desired energy range will be rejected on the basis of a coincidence requirement between the cesium-iodide scintillators, while those above and those which enter at an angle not acceptable to the telescope will be rejected by the output of the plastic scintillator.

2.3 HIGH-ENERGY DETECTOR SYSTEM

The detector system for particles of energy between 400 Mev and 10 Bev/nucleon is shown in cross section in Fig. 4. The first detector element is a 1/16-in. thick thallium-activated cesium-iodide energy loss rate scintillometer (detector 1) which provides information on the specific ionization of the incoming particle. The second detector element (detector 2) is a plastic coincidence crystal which defines the solid angle of the telescope such that only particles passing through this scintillator are counted. The third element of the detector is a Cerenkov radiator (detector 3). Output from this radiator is a function of the velocity and the square of the charge. Thus, the pulse from the energy loss rate scintillometer together with the pulse from the Cerenkov counter allow the determination of the particle charge and energy.

The basic data-handling circuitry for this detector system is the same

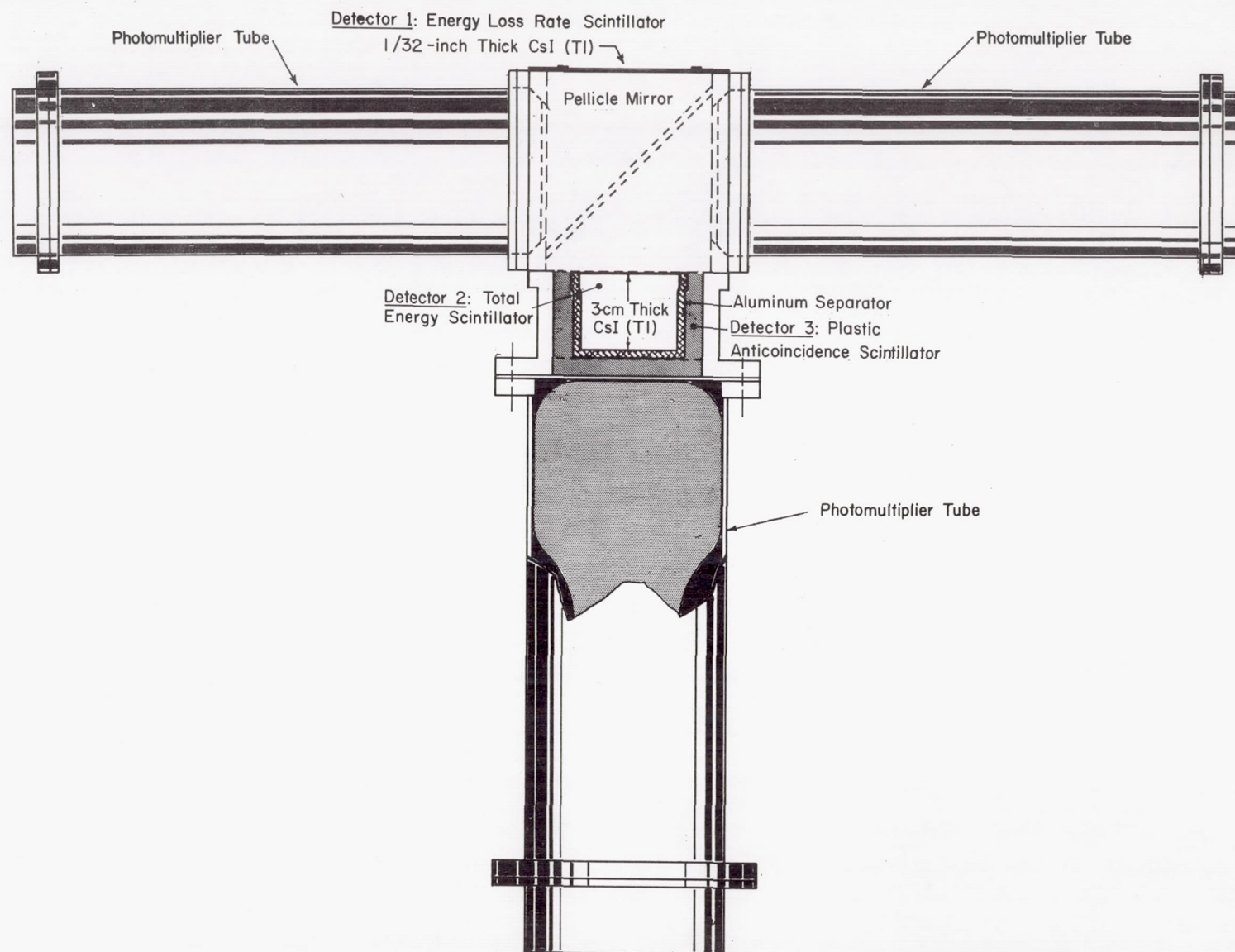


Figure 3. Cross-Sectional View of Low-Energy Detection System

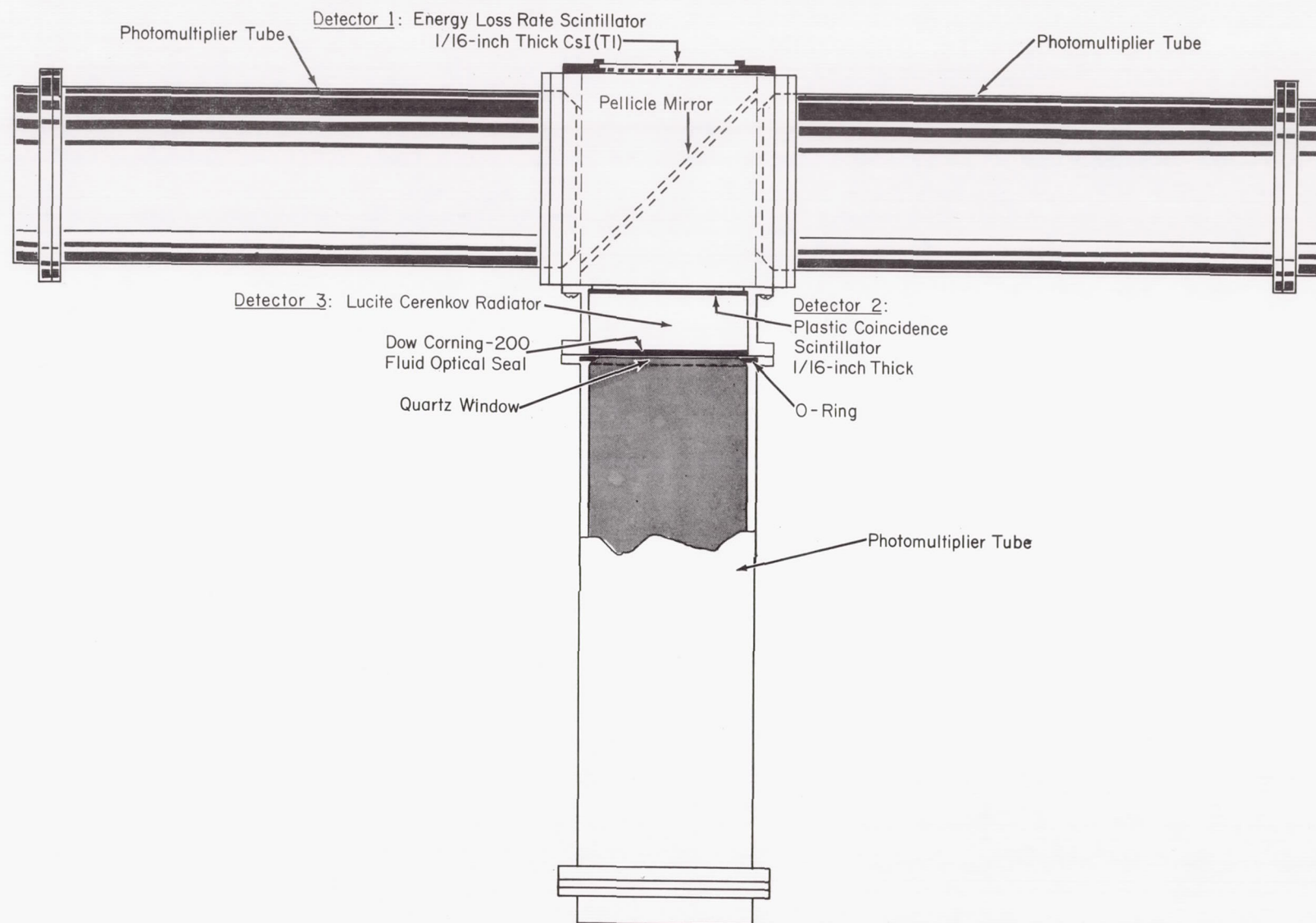


Figure 4. Cross-Sectional View of High-Energy Detection System

as for the low-energy system.

2.4 GOLD-SILICON DETECTORS

At the time work on this contract was begun, the available semiconductors had extremely small areas which precluded their use as heavy particle detectors because of the low density of the heavy component flux. However, in early 1960, Oak Ridge National Laboratories announced a gold-coated silicon semiconductor wafer having a surface barrier which could be made in a variety of sizes and shapes. That laboratory generously supplied samples of the detectors and information about their manufacture. The University then proceeded to adapt the detectors for the cosmic-ray program. These detectors* can be used to measure either total energy or energy loss rate. They possess better energy resolution capability than that usually obtainable from scintillator crystals and may have sufficient surface area to provide desirable data rates. Recent work at Oak Ridge and here at The University indicates that the effective thickness of the active depletion region may be varied as a function of applied voltage, allowing essentially the total bulk of the silicon wafer to be effective, if this is desired. Thickening the depletion layer raises the upper energy cutoff of the detector by providing a longer active ionizing path for signal contribution. For measuring total particle energy, it appears feasible to use the gold-silicon detector as a photodiode in the telescope.

The present indication is that the detector is capable of detecting a minimum of 20 to 30 Mev of energy loss within a CsI crystal. Thus it may be possible to replace the photomultiplier with a more rugged and less bulky element. Further work remains to be done in this area before a final choice may be made.

The height of the output pulse from the gold-silicon detector varies with the applied voltage and inversely with the area of the surface because of the detector's capacitance. Thus for use as a photodiode, a small detector should be efficiently coupled to a relatively large scintillator.

*Takaki, R., M. Perkins, and A. Tuzzolino: "A Gold-Silicon Surface-Barrier Proton Range Telescope." (to be published in the Proc. IRE).

Calculations of pulse-height as a function of detector area indicate that for the heavier nuclei the produced ion density is sufficient to allow use of relatively large-area detectors (several square cm) while retaining adequate signal-to-noise ratio for good pulse-height analysis.

The development of the AuSi detector has resulted in prototype instrumentation for the measurement of low-energy proton flux in the energy range 0.5 to 10 Mev. The first prototypes of those units were designed to provide a one and two channel capability. This restriction was due to the limitations in information storage capacity of current payloads. The first of these units was developed for flight in the Able-5B vehicle, * in which one digital word was made available from the two allocated to the cosmic-ray telescope. This instrument utilized a single AuSi detector in an epoxy mounting and was designed to cover the energy range from 0.5 to 10 Mev in one step. No performance information is available for space operation due to the failure of the Able-5B at launch. However, the type approval and acceptance tests of the unit did yield valuable data for the further improvement of the detector element for operation in a space environment.

Further development of detector fabrication and mounting techniques has led to a capability of providing a multielement range telescope consisting of a stacked series of AuSi detectors having little or no absorptive backing. With a two-element telescope of this type which has been developed for the Range vehicle ** it is now possible to obtain the proton flux over the energy range 0.5 to 5 Mev and 5 to 10 Mev, exclusive of electron and gamma background.

Flight models of the two instruments described above are shown in Figs. 5 and 6. Detailed operational characteristics of the instruments have been presented in previous quarterly reports (LAS-QR-E165-5 and 6).

The use of the AuSi detector in applications where pulse-height analysis is possible offers a number of advantages. Figure 7 shows the energy resolution capability of a representative detector fabricated at the University. An alpha-particle source composed of 10% Cm²⁴² and 90% Cm²⁴⁴ was used

* Flight instrumentation for the Able-5B was prepared under Contract No. NASw-24.

** Flight instrumentation is being provided under separate funding for the Ranger vehicles.

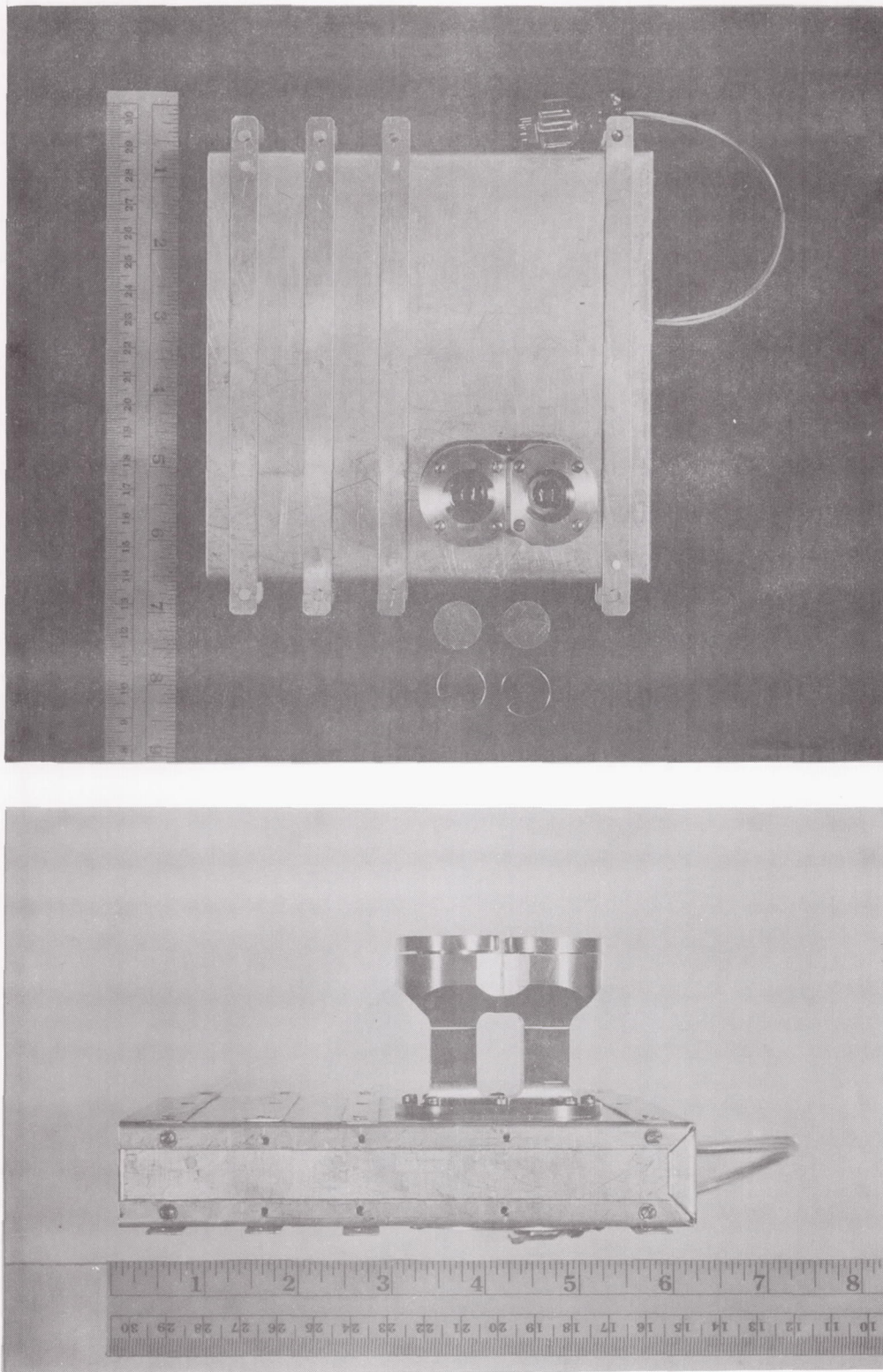


Figure 5. Resultant Type Approval Unit for Able-5 Instrumentation

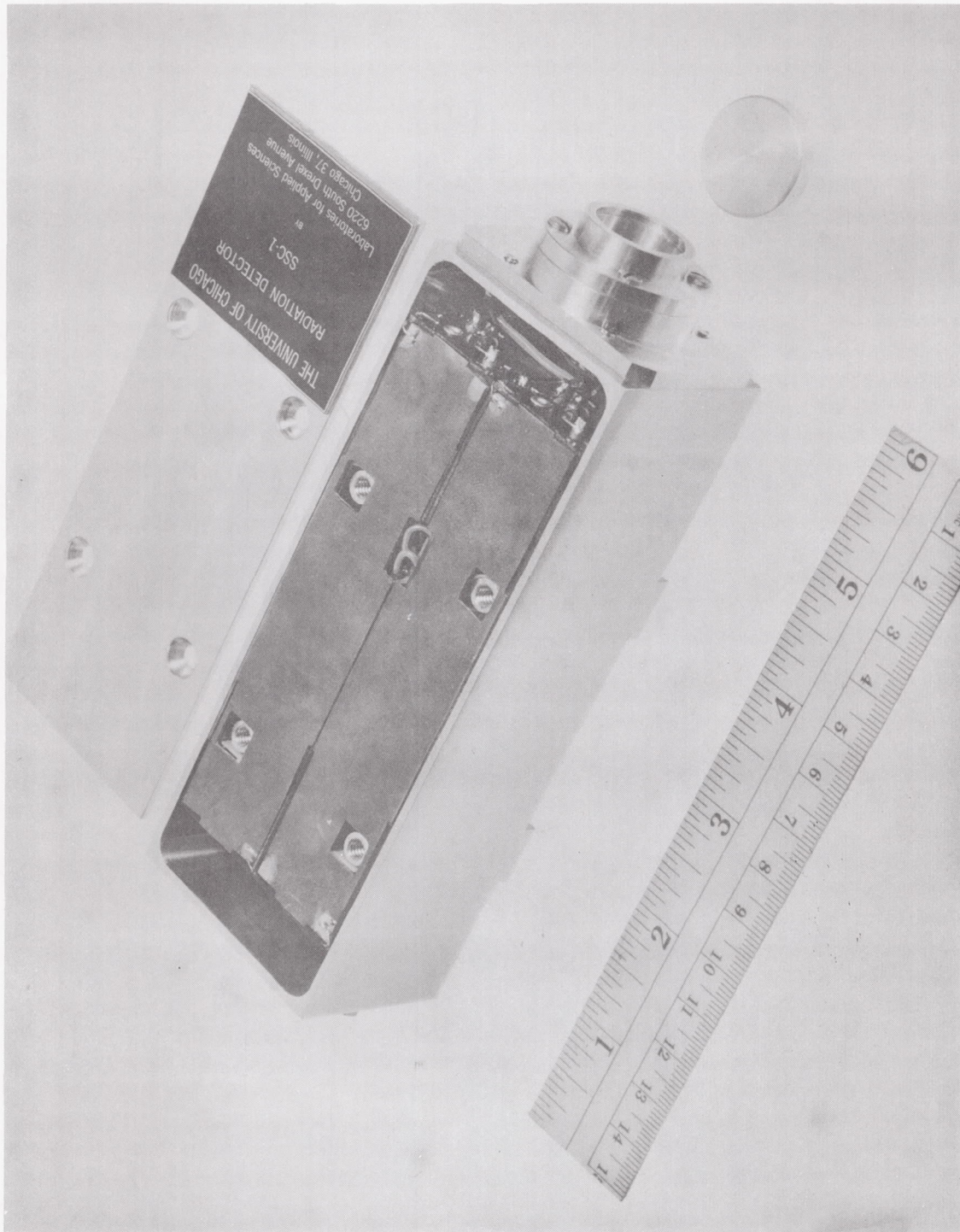


Figure 6. Instrument Configuration

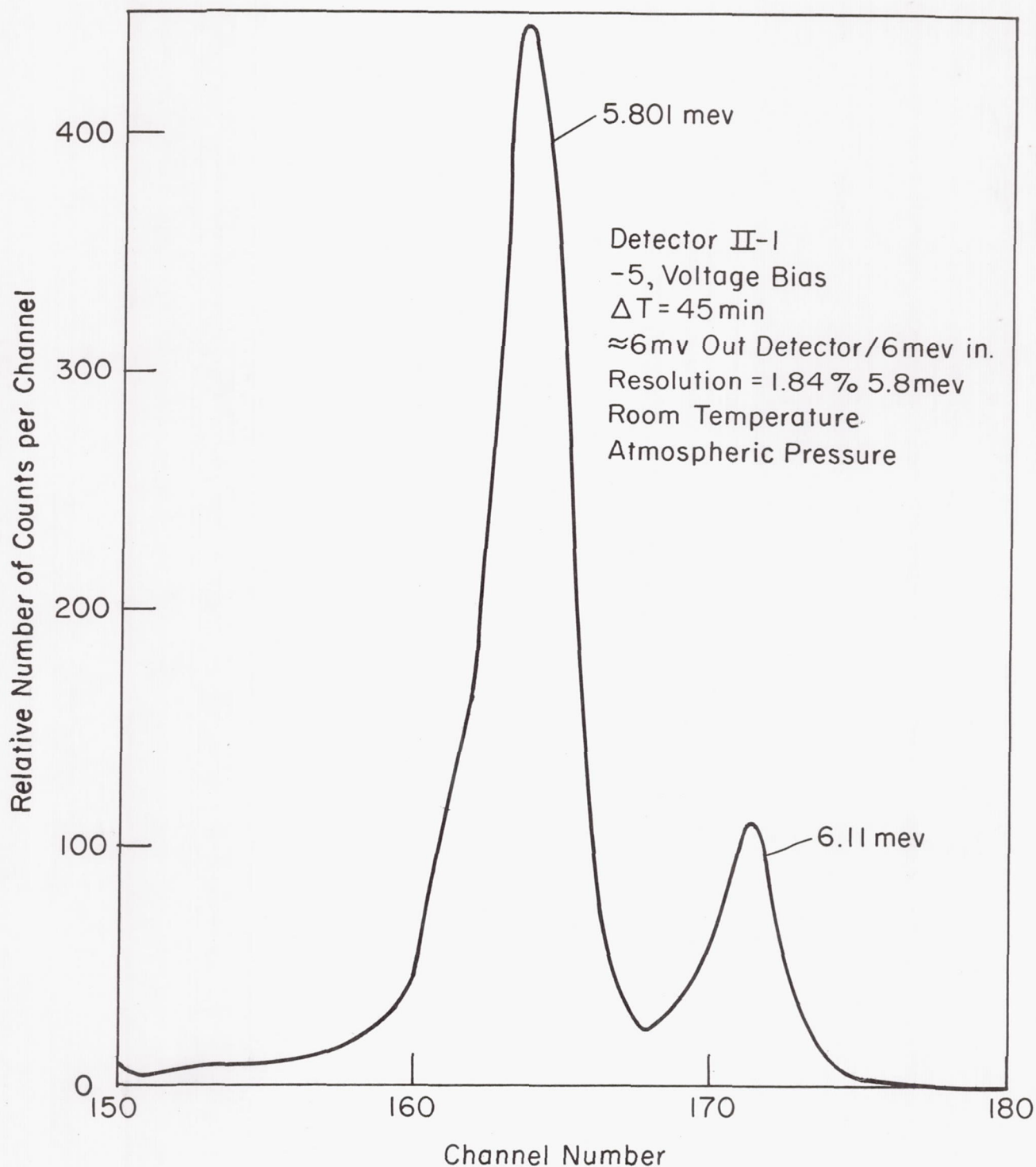


Figure 7. Energy Resolution for Gold-Silicon Solid State Detector

to obtain this curve, which represents a capability in excess of that presently maintained in the electronic circuitry. It has been possible to obtain even better resolution in many other cases.

3. DATA HANDLING

3.1 PULSE-HEIGHT ANALYSIS

Concurrently with the detector development, pulse-height analysis circuitry suitable for satellite use was developed. The first effort produced a circuit containing germanium components for use in the balloon-borne tests. Subsequent effort has been toward an orderly transfer to circuitry utilizing silicon components to achieve thermal stability over a greater range and a minimum loss in system speed.

Each detection system requires two channels of pulse-height analysis—one for each of the first two crystals. The block diagram of the circuitry associated with the low-energy detector system is illustrated in Fig. 8. The output of detectors 1 and 2 for the low-energy unit represents the energy loss rate and total energy scintillometers, respectively, while detector 3 is the anticoincidence limiter for the system.

In the low-energy detection system the pulses produced by detectors 1 and 2 are applied to the respective preamp-range switch combinations shown in Fig. 9. If either or both of the pulses exceed a predetermined level, then the range switch in the appropriate channel, or channels, is activated to attenuate the pulse, thus extending the dynamic range of the system.

The pulses are then passed from the preamp-range switch through electronic gates which are normally set to pass signals. Outputs from the respective gates are then applied to the parallel channels of the pulse-height analyzer, and also into identical discriminator circuits. The trigger sensitivities of the discriminators establish the minimum pulse height to which the system will respond. The two discriminators feed a coincidence circuit in which an output will occur only if the inputs are coincident in time. The coincidence pulse is then coupled through an anticoincidence gate to the 15-microsecond one-shot multivibrator. This gate will pass the coincidence pulse unless there should also be a pulse occurring at the output of detector 3. Thus, if there is an output from detectors 1 and 2, but not 3, the 15-microsecond one-shot multivibrator will be triggered. This one-shot multivibrator, therefore, sets the width of a pulse-stretching circuit in the pulse-height analyzer. It will be noted that an output

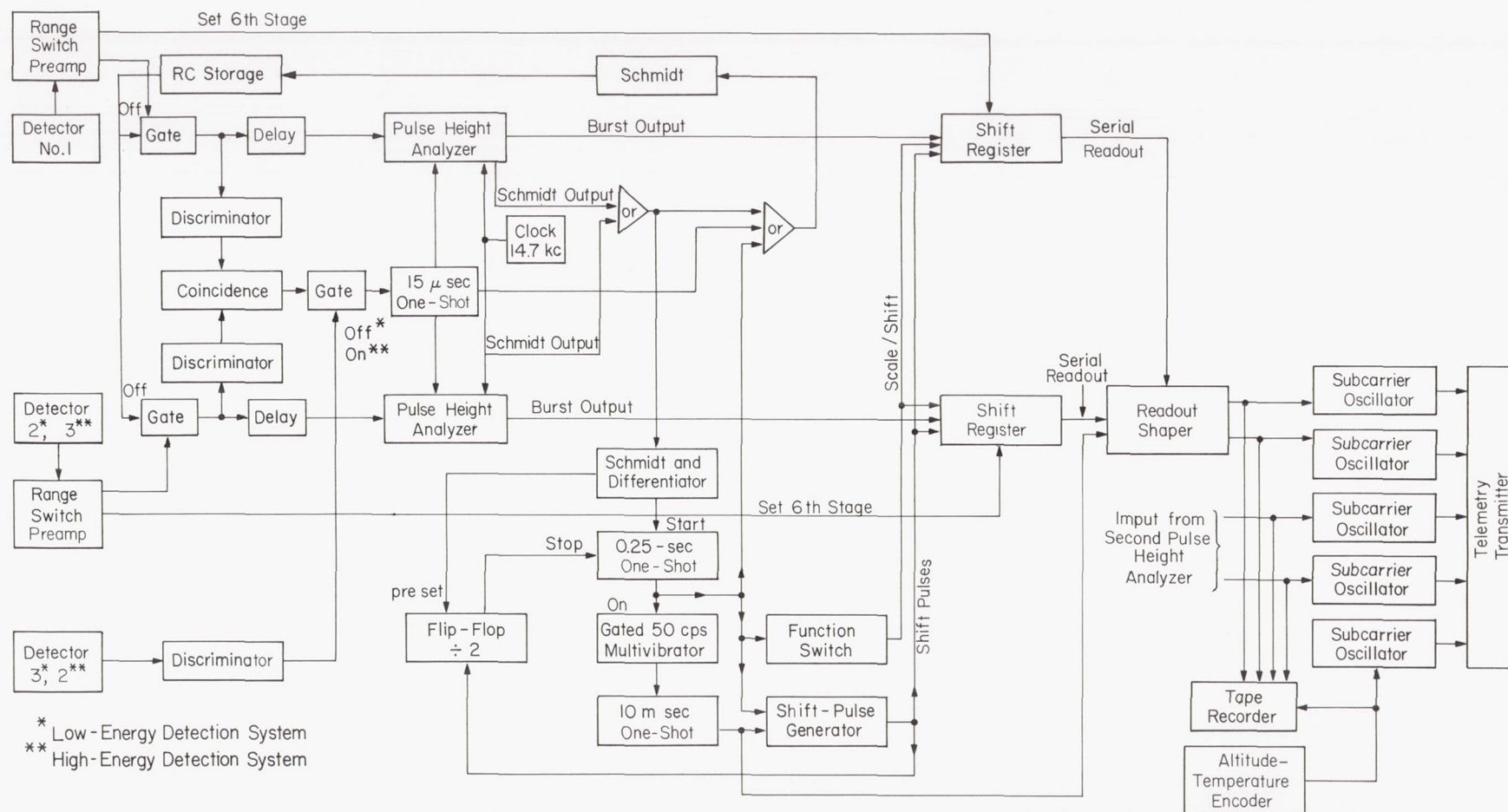
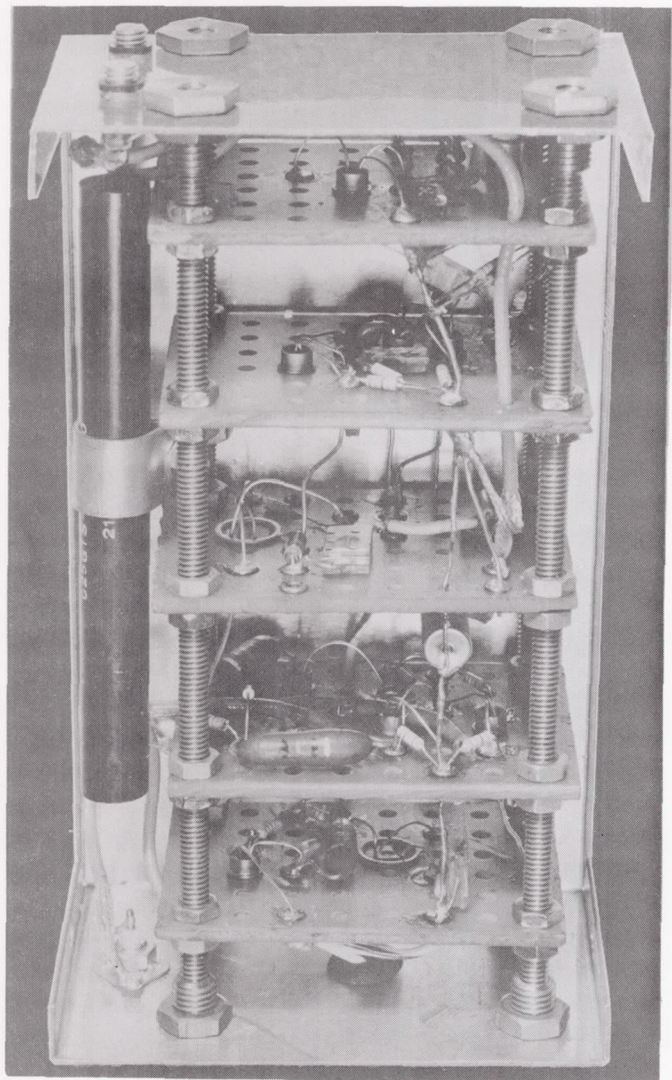
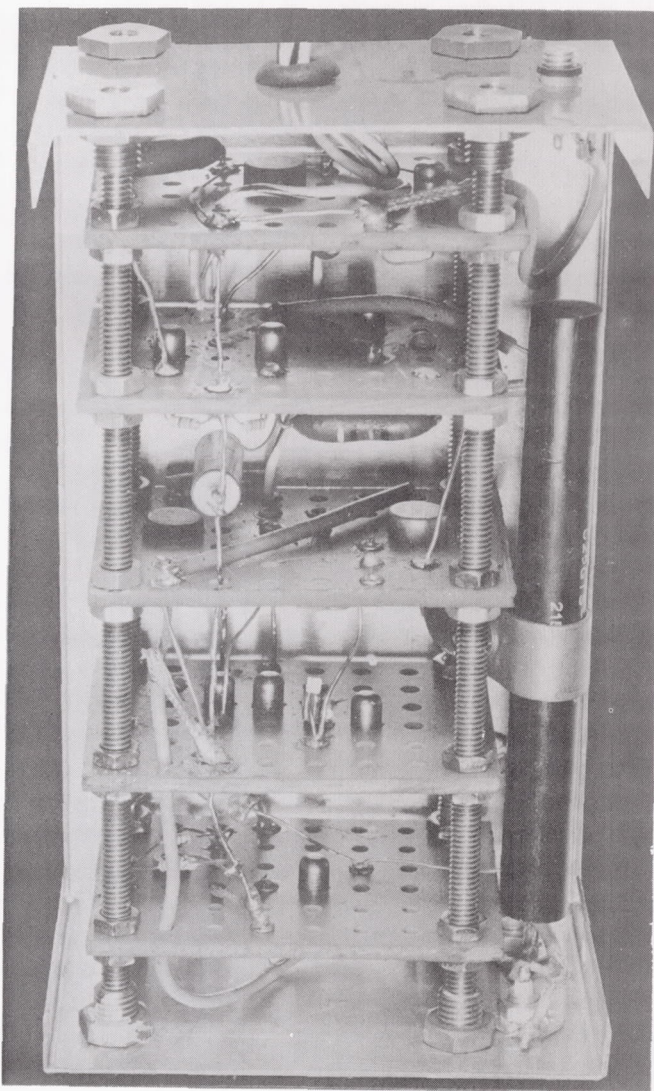


Figure 8. Block Diagram of System for the Monitoring of Low-Energy Cosmic Ray Primaries



Top View



Bottom View

Figure 9. Preamp and Range Switch Assembly

of the one-shot multivibrator is also applied through an "or" circuit to change the state of a Schmidt trigger circuit which serves to gate-off the inputs to channels 1 and 2, thus preventing any further pulses from entering the system during the 15-microsecond interval.

The signal pulses have been applied to a pulse-stretching circuit through a $1/2$ -microsecond delay line to ensure that the 15-microsecond pulse has reached essentially full voltage prior to the application of the signal pulse. The stretched pulses have an amplitude proportional to the input pulse and a duration of approximately 15-microseconds. During the interval of the stretched pulse, a precision capacitor is charged to the voltage level of the stretched pulse. The circuit in which this is accomplished employs transistors as switching elements. At the end of the 15-microsecond interval the capacitor is switched into a discharge circuit to produce an essentially linear ramp function. The abrupt step at the leading edge of the ramp changes the state of another Schmidt trigger circuit which recovers as the ramp function passes through the reset level. The duration of the rectangular pulse produced by the trigger circuit is governed entirely by the height of the ramp which, in turn, is directly proportional to the height of the original signal pulse, thus providing a conversion from pulse height to time.

This rectangular pulse is used to gate a timing oscillator. All pulses occurring in a given burst are stored in a 5-place binary scaler permitting identification of 31 increments in pulse height. As mentioned previously, the range switches are used to extend the dynamic range of the system. If the range switch in either channel is activated, then the sixth bit in the binary scaler is set to read 1; otherwise, a zero. The range switches act to give the equivalent of 63 channels of analysis. Since the two channels will generally be analyzing different pulse heights, the counting times required will differ.

The outputs of the two Schmidt trigger circuits, one in each channel, are combined in an "or" circuit to provide a signal which (1) starts when the 15-microsecond pulse-stretching interval ends and (2) ends when the longest count is registered. This "count gate" pulse is applied to the input squelch gate to maintain the input circuitry in the "off" state throughout the combined counting intervals.

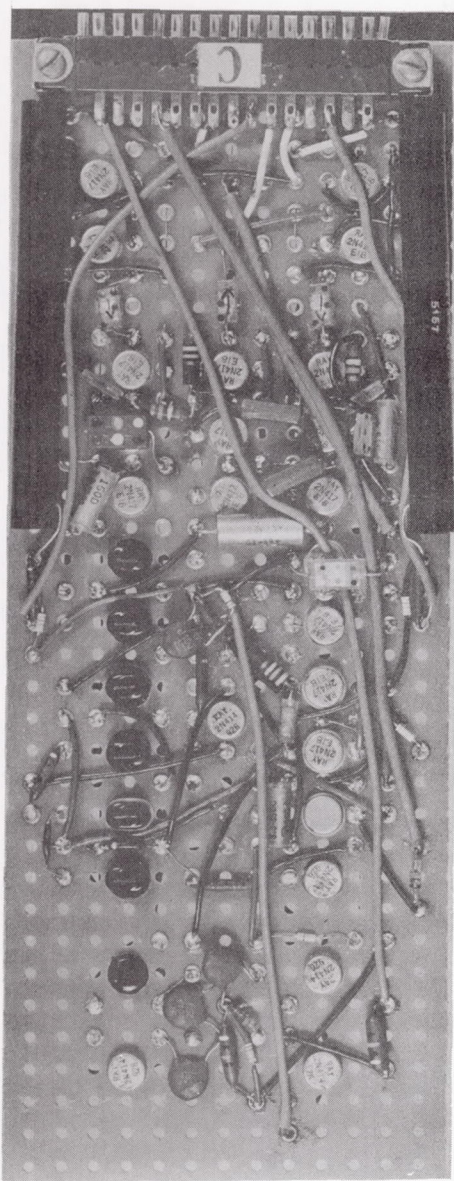
The count gate pulse is differentiated and its trailing edge is used to start the readout cycle. This trailing edge pulse triggers a $1/4$ -second one-shot circuit. The output of the one-shot circuit is also applied to the input squelch gate. Thus, the input circuit continues in the "off" state during

the readout cycle. An additional function of the one-shot circuit's output is the gating-on of the shift pulse generator. The first shift pulse occurs 30-milliseconds after counting is completed, and subsequent shift pulses occur at 20-millisecond intervals thereafter. Since a minimum of six shift pulses is required, provision is included to reset the 1/4-second one-shot circuit when the eighth shift pulse appears to gate-off the shift pulse oscillator. Two extra shift pulses are sent in order to assure that the storage registers are shifted out completely. The shift pulse frequency is divided by a factor of two in a conventional flip-flop circuit. Providing the flip-flop was in the proper state before the first shift pulse, the output will consist of pulses coinciding with the even-numbered shift pulses. These are added to the normal exponential decay wave in the one-shot circuit such that the forth pulse (corresponding to the eighth shift pulse) will drive the cutoff stage into conduction. Although this could be accomplished using the shift pulses directly, division by two permits a considerably wider latitude in supply voltage and circuit parameters. In a voltage variation test, perfect stability was retained over a $\pm 30\%$ range of supply voltages.

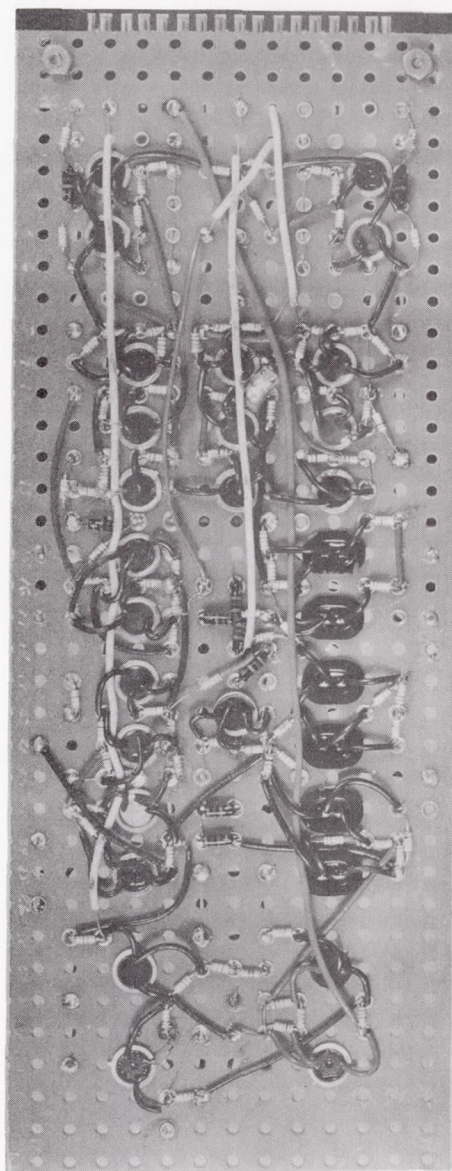
Figure 10 shows the programmer board. This board contains the "or" circuit controlling the input gates, the 15-microsecond one-shot multivibrator, the 1/4-second gated 50-cps readout multivibrator, the shift pulse generator, and the function switch. Figure 11 shows the height-to-time converter board.

As previously mentioned, it is essential that the flip-flop circuit be in the proper state when the first shift pulse occurs. To ensure that this is always the case, a pulse derived from the leading edge of the "count gate" is applied to one side of the flip-flop to serve as a preset pulse.

The output of the shift register is applied through the readout shaper to an on-board tape recorder and to the telemetry subcarrier oscillator such that the signal is composed of eight digits which are either 0 or 1. A third reference level is used during the time that the shift register is inoperative. Thus, the start of a telemetered message is indicated by a shift in subcarrier oscillator frequency from a reference level to a 0 or 1 followed by a succession of 5 additional digits which are either 0 or 1 depending upon the pulse-height analysis and, finally, two more 0's for check purposes. The binary number which is produced by the readout shift register is an indication of the condition of the 31-channel pulse-height analyzer and the range switch as a result of the particular signal and is thus a measure of pulse height. It is this

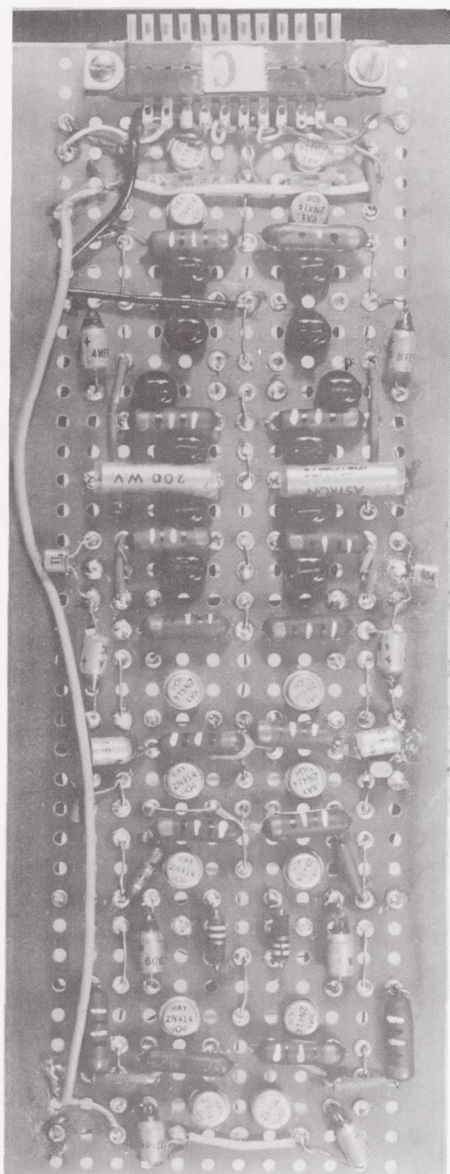


Top View

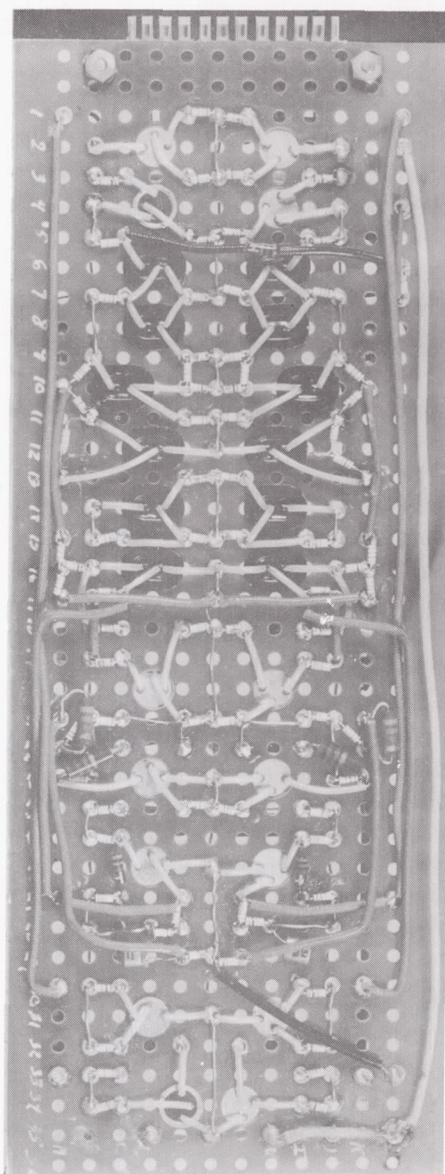


Bottom View

Figure 10. Programmer Board



Top View



Bottom View

Figure 11. Height-to-Time Convertor Board

form of data which must be reduced to obtain energy and atomic number of the incoming particle. Figure 12 shows the readout board which contains the shift register, the serial readout, the crystal clock, and the readout shaper.

The above is a description of the low-energy unit; however, the high-energy detector system is identical except that detector 2 acts as a coincidence crystal rather than as an anticoincidence crystal; i.e., the pulses from detectors 1 and 3 are analyzed only if the particle passes also through detector 2.

3.2 DATA RATE

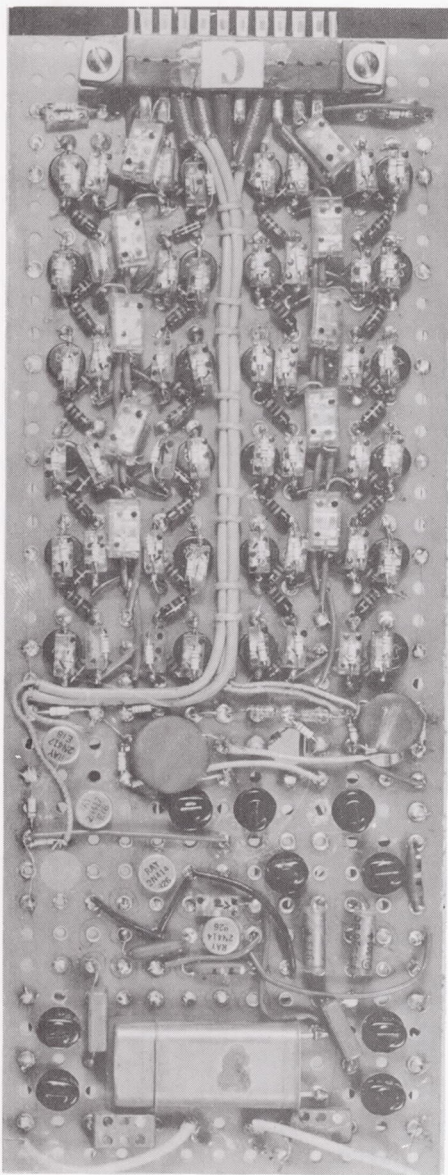
Because the information band width of present satellite communication systems is narrow, it was necessary to study the techniques for on-board computation and storage of the large number of information bits. In the present LAS system design, each cosmic-ray event is characterized by a 14-bit data word. At the expected rate of 3 to 5 events per minute, the required continuous transmission rate for radiation would be a minimum of 42 bits per minute.

3.3 ANALYSIS AND GROUPING OF COSMIC RAY PARTICLES

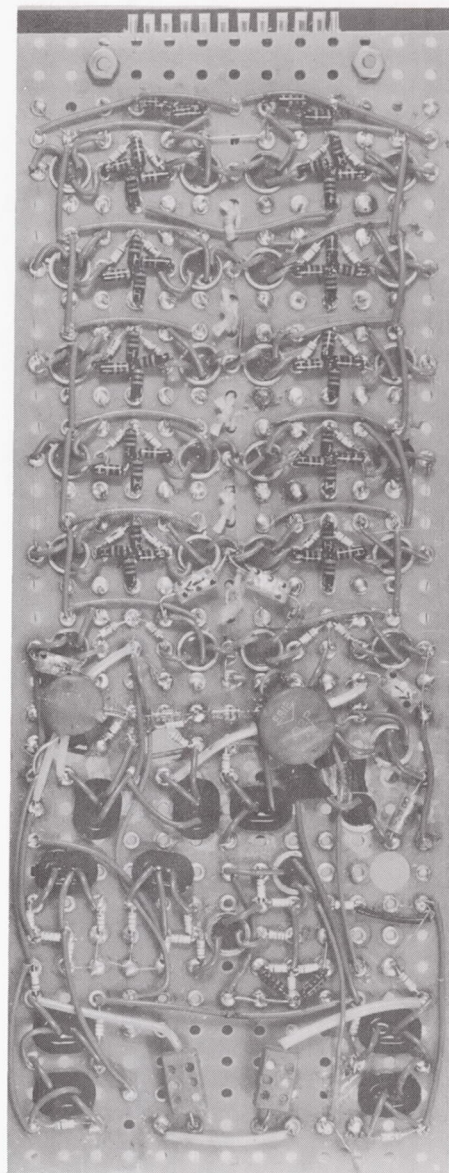
3.3.1 DETECTION RANGE FOR LOW-ENERGY DETECTOR

The detection range of the low-energy detector for cosmic ray primaries is determined by the physical parameters of the detector. The detection capability may be obtained from the energy-range tables, Tables 1 and 2. The absorption thickness of the total energy scintillator is 13.53 gms/cm^2 . From Table 1 it may be determined that the low-energy detector will resolve energies for carbon-12 ions between 50 and 200 Mev/nucleon and iron-56 ions between 63 and 500 Mev/nucleon. All particles with a range less than 0.269 gm/cm^2 of phenyl-cyclohexane will be rejected by the coincidence requirement between the two cesium-iodide scintillator crystals. The particles of range greater than 9.00 gms/cm^2 of phenyl-cyclohexane will be rejected through use of the plastic scintillator (see Fig. 3) which is in anti-coincidence with the two cesium-iodide crystals.

Computation of the data-handling requirements of the system may be made by reference to Tables 1 and 2. Consider first the range of pulse heights



Top View



Bottom View

Figure 12. Shift Register and Readout Board

Table 1. Range in Phenyl-Cyclohexane (gm/cm²)

Atomic No.	Element	Range (gm/cm ²)																							
Energy of Incoming Particle (mev/nucleon) → 50		63	80	100	125	160	200	250	320	400	500	630	800	1000	1250	1600	2000	2500	3200	4000	5000	6300	8000	10000	
1	H ¹	2.14	3.25	5.00	7.45	11.1	17.2	25.2	36.8	61.5	80.0	114.	162.	231	317	432	595	784	1023	1360	1737	2202	2800	3549	4415
2	He ⁴	2.14	3.25	5.00	7.45	11.1	17.2	25.2	36.8	61.5	80.0	114.	162.	231	317	432	595	784	1023	1360	1737	2202	2800	3549	4415
3	Li ⁷	1.66	2.53	3.89	5.80	8.62	13.4	19.6	28.6	47.8	62.2	88.6	126.	180	247	336	463	610	796	1058	1351	1713	2178	2761	3435
4	Be ⁹	1.20	1.83	2.81	4.19	6.23	9.67	14.1	20.7	34.6	45.0	64.0	91.0	130	178	243	334	441	574	764	976	1238	1574	1995	2481
5	B ¹¹	0.942	1.43	2.20	3.28	4.88	7.57	11.1	16.2	27.1	35.2	50.1	71.3	102	140	190	262	345	450	598	764	969	1232	1562	1943
6	C ¹²	0.713	1.08	1.66	2.48	3.69	5.73	8.38	12.3	20.5	26.6	38.0	53.9	77.0	106	144	198	261	341	453	578	733	932	1182	1470
7	N ¹⁴	0.612	0.930	1.43	2.13	3.17	4.92	7.20	10.5	17.6	22.9	32.6	46.3	66.1	90.8	124	170	224	293	389	497	630	801	1015	1263
8	O ¹⁶	0.535	0.813	1.25	1.87	2.77	4.30	6.29	9.20	15.4	20.0	28.5	40.5	57.8	79.4	108	149	196	256	340	434	551	700	887	1104
9	F ¹⁹	0.503	0.764	1.18	1.75	2.60	4.04	5.91	8.65	14.4	18.8	26.8	38.1	54.3	74.6	102	140	184	240	320	408	517	658	834	1038
10	Ne ²⁰	0.428	0.650	1.00	1.49	2.22	3.44	5.03	7.36	12.3	16.0	22.8	32.4	46.2	63.5	86.4	119	157	205	272	347	440	560	710	883
11	Na ²³	0.407	0.618	0.950	1.42	2.11	3.27	4.78	7.00	11.7	15.2	21.6	30.8	43.9	60.3	82.1	113	149	194	258	330	418	532	674	839
12	Mg ²⁴	0.357	0.543	0.835	1.24	1.85	2.87	4.20	6.15	10.3	13.4	19.0	27.1	38.6	53.0	72.1	99.4	131	171	227	290	368	468	593	737
13	Al ²⁷	0.342	0.520	0.800	1.19	1.77	2.75	4.03	5.89	9.84	12.8	18.2	25.9	37.0	50.8	69.1	95.2	125	164	218	278	352	448	568	706
14	Si ²⁸	0.306	0.465	0.715	1.06	1.58	2.46	3.60	5.26	8.79	11.4	16.3	23.2	33.1	45.3	61.8	85.1	112	146	194	248	315	400	508	631
15	P ³¹	0.295	0.449	0.690	1.03	1.53	2.37	3.47	5.08	8.49	11.0	15.7	22.4	31.9	43.8	59.6	82.1	108	141	188	240	304	386	490	609
16	S ³²	0.268	0.406	0.625	0.931	1.38	2.15	3.15	4.60	7.69	10.0	14.2	20.2	28.9	39.7	54.0	74.4	98.0	128	170	217	275	350	444	552
17	Cl ³⁵	0.259	0.393	0.605	0.901	1.34	2.08	3.04	4.46	7.44	9.68	13.8	19.6	28.0	38.4	52.3	72.0	94.9	124	165	210	266	339	429	534
18	A ⁴⁰	0.263	0.400	0.615	0.916	1.36	2.12	3.10	4.53	7.56	9.84	14.0	19.9	28.4	39.0	53.1	73.2	96.4	126	167	214	271	344	437	543
19	K ³⁹	0.231	0.351	0.540	0.805	1.20	1.86	2.72	3.98	6.64	8.64	12.3	17.5	25.0	34.3	46.7	64.3	84.7	110	147	188	238	302	383	477
20	Ca ⁴⁰	0.214	0.325	0.500	0.745	1.11	1.72	2.52	3.68	6.15	8.00	11.4	16.2	23.1	31.7	43.2	59.5	78.4	102	136	174	220	280	355	442
21	Sc ⁴⁵	0.218	0.332	0.510	0.760	1.13	1.75	2.57	3.76	6.27	8.16	11.6	16.5	23.5	32.4	44.1	60.7	80.0	104	139	177	225	286	362	450
22	Ti ⁴⁸	0.212	0.322	0.496	0.739	1.10	1.71	2.50	3.65	6.10	7.94	11.3	16.1	22.9	31.5	42.8	59.0	77.8	101	135	172	218	278	352	438
23	V ⁵¹	0.206	0.314	0.482	0.719	1.07	1.66	2.43	3.55	5.93	7.72	11.0	15.6	22.3	30.6	41.7	57.4	75.7	99	131	168	212	270	342	426
24	Cr ⁵²	0.193	0.293	0.452	0.673	1.00	1.55	2.27	3.32	5.55	7.22	10.3	14.6	20.9	28.7	39.0	53.7	70.8	92	123	157	199	253	320	399
25	Mn ⁵⁵	0.188	0.286	0.440	0.656	0.975	1.51	2.21	3.24	5.41	7.04	10.0	14.3	20.3	28.2	38.0	52.4	69.0	90	120	153	194	246	312	389
26	Fe ⁵⁶	0.177	0.269	0.414	0.618	0.918	1.42	2.09	3.05	5.10	6.63	9.44	13.4	19.2	26.3	35.8	49.3	65.0	85	113	144	183	232	294	366
27	Co ⁵⁹	0.173	0.263	0.404	0.603	0.896	1.39	2.04	2.98	4.98	6.47	9.21	13.1	18.7	25.7	34.9	48.1	63.4	83	110	141	178	227	287	357
28	Ni ⁵⁸	0.160	0.240	0.370	0.551	0.820	1.27	1.86	2.72	4.55	5.92	8.43	12.0	17.1	23.5	32.0	44.0	58.0	76	101	129	163	207	263	327
29	Cu ⁶³	0.160	0.244	0.375	0.559	0.831	1.29	1.89	2.76	4.61	6.00	8.54	12.2	17.3	23.8	32.4	44.6	58.8	77	102	130	165	210	266	331
30	Zn ⁶⁴	0.152	0.231	0.356	0.530	0.788	1.22	1.79	2.62	4.37	5.69	8.10	11.5	16.4	22.6	30.7	42.3	55.7	73	97	124	157	199	252	314
31	Ga ⁶⁹																								
Range, R (gm/cm ²) →		R < 0.25	0.25 < R < .5	0.5 < R < 1.0	1.0 < R < 2.0	2.0 < R < 4.0	4.0 < R < 8.0	8.0 < R < 16.0	16.0 < R < 32.0																

Range, R (gm/cm²) → R < 0.25 0.25 ≤ R < .5 0.5 ≤ R < 1.0 1.0 ≤ R < 2.0 2.0 ≤ R < 4.0 4.0 ≤ R < 8.0 8.0 ≤ R < 16.0 16.0 ≤ R < 32.0

Table 2. Rate of Energy Loss in Matter Referred to Phenyl-Cyclohexane

Atomic No.	Element	Rate of Energy Loss (mev/gm-cm ²)																							
Energy of Incoming Particle (mev/nucleon) → 50		63	80	100	125	160	200	250	320	400	500	630	800	1 BeV	1.25	1.60	2.00	2.50	3.20	4.00	5.00	6.30	8.00	10.0	
1	H ¹	12.9	10.72	8.90	7.51	6.38	5.37	4.62	4.02	3.49	3.11	2.81	2.58	2.38	2.26	2.18	2.12	2.08	2.09	2.10	2.13	2.17	2.22	2.28	2.34
2	He ⁴	51.6	42.88	35.60	30.04	25.6	21.5	18.5	16.1	14.0	12.4	11.2	10.3	9.52	9.04	8.70	8.46	8.32	8.34	8.41	8.52	8.68	8.88	9.12	9.36
3	Li ⁷	106.1	96.48	80.10	67.59	57.4	48.3	41.6	36.2	31.4	28.0	25.3	23.2	21.4	20.3	19.6	19.0	18.7	18.8	18.9	19.2	19.5	20.0	20.5	21.1
4	Be ⁹	206	171.5	142.40	120.16	102.1	85.9	73.9	64.3	55.8	49.8	45.0	41.3	38.1	36.2	34.8	33.8	33.3	33.4	33.6	34.1	34.7	35.5	36.5	37.4
5	B ¹¹	322	268.0	222.5	187.8	160	134	116	100.5	87.3	77.8	70.3	64.5	59.5	56.5	54.4	52.9	52.0	52.2	52.6	53.3	54.3	55.5	57.0	58.5
6	C ¹²	464	385.9	320.4	270.4	230	193	166	145	126	112	101	92.9	85.7	81.4	78.3	76.1	74.9	75.1	75.7	76.7	78.1	79.9	82.1	84.2
7	N ¹⁴	632	525.3	436.1	368.0	313	263	226	197	171	152	138	126	117	111	107	104	102	103	104	106	109	112	115	118
8	O ¹⁶	826	686.1	569.6	480.6	408	344	296	257	223	199	180	165	152	145	139	135	133	134	135	136	139	142	146	150
9	F ¹⁹	1045	868.3	720.9	608.3	517	435	374	326	283	252	228	209	193	183	176	171	168	169	170	173	176	180	185	190
10	Ne ²⁰	1290	1072	890.0	751.0	638	537	462	402	349	311	281	258	238	226	218	212	208	209	210	213	217	222	228	234
11	Na ²³	1561	1297	1077	909.0	772	650	559	486	422	376	340	312	288	273	263	256	252	252	254	258	263	269	276	283
12	Mg ²⁴	1858	1544	1282	1081	919	773	665	579	503	448	405	372	343	325	313	305	300	300	303	307	312	320	328	337
13	Al ²⁷	2180	1812	1504	1269	1078	908	781	679	590	526	475	436	402	382	368	357	352	353	355	360	367	375	385	395
14	Si ²⁸	2528	2101	1744	1472	1250	1053	906	788	684	610	551	506	466	443	426	415	408	409	412	417	425	435	447	459
15	P ³¹	2903	2412	2003	1690	1436	1208	1040	905	785	700	632	581	536	509	490	476	468	469	473	479	488	500	513	527
16	S ³²	3302	2744	2278	1923	1633	1375	1183	1029	893	796	719	660	609	579	557	541	532	534	538	545	556	568	584	599
17	Cl ³⁵	3728	3098	2572	2170	1844	1552	1335	1162	1009	899	812	746	688	653	629	611	601	603	607	616	627	642	659	676
18	Ar ⁴⁰	4180	3473	2884	2433	2067	1740	1497	1302	1131	1008	910	836	771	732	705	685	674	676	681	690	703	719	739	758
19	K ³⁹	4657	3870	3213	2711	2303	1939	1668	1451	1260	1123	1014	931	859	816	786	764	751	753	759	769	783	801	823	845
20	Ca ⁴⁰	5160	4288	3560	3004	2552	2148	1848	1608	1396	1244	1124	1032	952	904	870	846	832	834	841	852	868	888	912	936
21	Sc ⁴⁵	5689	4728	3925	3312	2814	2368	2037	1773	1539	1372	1239	1138	1050	997	960	933	917	920	927	939	957	979	1005	1032
22	Ti ⁴⁸	6244	5188	4308	3635	3088	2599	2236	1946	1689	1505	1360	1249	1152	1093	1053	1024	1007	1010	1017	1031	1050	1074	1104	1133
23	V ⁵¹	6824	5671	4708	3973	3375	2841	2444	2127	1846	1645	1486	1365	1259	1196	1151	1119	1100	1103	1112	1127	1148	1174	1206	1238
24	Cr ⁵²	7430	6175	5126	4326	3675	3093	2661	2316	2010	1791	1619	1486	1371	1302	1253	1218	1198	1202	1211	1227	1250	1279	1313	1348
25	Mn ⁵⁵	8063	6700	5563	4694	3988	3356	2888	2513	2181	1944	1756	1613	1488	1413	1360	1322	1300	1304	1314	1331	1356	1388	1425	1463
26	Fe ⁵⁶	8720	7247	6016	5077	4313	3630	3123	2718	2359	2102	1900	1744	1609	1528	1471	1430	1406	1410	1421	1440	1467	1501	1541	1582
27	Co ⁵⁹	9404	7815	6488	5475	4651	3915	3368	2931	2544	2267	2048	1881	1735	1648	1586	1542	1516	1521	1532	1553	1582	1618	1662	1706
28	Ni ⁵⁸	10,114	8404	6978	5888	5002	4210	3622	3152	2736	2438	2203	2023	1866	1772	1706	1658	1631	1635	1648	1670	1701	1740	1788	1835
29	Cu ⁶³	10,849	9016	7485	6316	5366	4516	3885	3381	2935	2616	2363	2170	2002	1901	1830	1779	1749	1754	1768	1791	1825	1867	1917	1968
30	Zn ⁶⁴	11,610	9648	8010	6759	5742	4833	4158	3618	3141	2799	2529	2322	2142	2034	1958	1904	1872	1877	1892	1917	1953	1998	2052	2106
31	Ga ⁶⁹																								
Range, R (gm/cm ²)→		R < 0.25	0.25 < R < .5	0.5 < R < 1.0	1.0 < R < 2.0	2.0 < R < 4.0	4.0 < R < 8.0	8.0 < R < 16.0	16.0 < R < 32.0																

Range, R (gm/cm²) → R < 0.25 0.25 ≤ R < .5 0.5 ≤ R < 1.0 1.0 ≤ R < 2.0 2.0 ≤ R < 4.0 4.0 ≤ R < 8.0 8.0 ≤ R < 16.0 16.0 ≤ R < 32.0

that will be produced in the energy loss rate scintillator. The smallest pulse will be produced by a carbon-12 nucleus of 200 Mev/nucleon. The largest pulse will be produced by an iron-56 particle of 63 Mev/nucleon. Calculations show that the largest pulse is approximately 43.7 times larger than the smallest pulse. This dynamic range is then divided into 64 increments by the pulse-height analysis system.

For the total energy scintillator in the low-energy system, the smallest pulse is produced by a carbon-12 nucleus of 50 Mev/nucleon while the largest pulse is produced by an iron-56 nucleus of 500 Mev/nucleon. Calculations show the dynamic range to be 56.0 to 1. This range can easily be handled by the analysis system.

3.3.2 DETECTION RANGE FOR HIGH-ENERGY DETECTOR

The detection range of the high-energy detection system may be determined in a similar way. The absorption thickness of the energy loss rate scintillator is 0.716 gm/cm^2 , since the scintillator is just twice as thick (1/16 inch) as the corresponding crystal on the low-energy detector (1/32 inch). The smallest pulse will be produced by a carbon-12 nucleus at 2 Bev/nucleon and the largest pulse is produced by an iron-56 nucleus at 400 Mev/nucleon. Calculations show that the largest pulse is 28.0 times greater than the smallest pulse. Again the analyzer can easily handle this dynamic range.

For the Cerenkov counter, the smallest pulse is produced by a carbon-12 nucleus of 400 Mev/nucleon. Since the Cerenkov pulse has the form of $K(1 - 1/n^2\beta^2)$, where n is the index of refraction of the material and β is the ratio of the particle velocity to the velocity of light, $n\beta$ must be ≥ 1 . Because n is 1.5 for Lucite, the Cerenkov radiator material, β must be greater than 2/3, or 0.67. A particle of 400 Mev/nucleon has a β of 0.71. Thus, the figure of $\beta = 0.71$ or 400 Mev/nucleon was chosen as a suitable value for the minimal pulse, in view of the fact that the low-energy detector covers the range up to 500 Mev/nucleon. The smallest pulse is produced by a carbon-12 nucleus of 400 Mev/nucleon. The largest pulse is produced by an iron-56 particle of 2.0 Bev/nucleon. This particle has a β of 0.95. Calculations show that the largest pulse is 85 times larger than the smallest pulse. This dynamic range can readily be handled by the analysis system.

4. FLIGHT TESTS

The equipment described above using the cesium iodide scintillators and Cerenkov radiators was flown on balloons under contract to the Aeromedical Field Laboratory of Holloman Air Force Base. The flights provided a test of system operation in the high-altitude (120,000 ft.) environment and also provided a means not otherwise available for obtaining a heavy particle flux in the energy range for which the instrumentation was designed.

A representative list of recorded events for which assignments could be made from one of the balloon flights is given in Table 3. These events were obtained from a flight from International Falls, Minnesota on 19 August 1959. As seen from the table, there were 10 events in the Li, Be, B group, 8 events in the C, N, O, F group, 5 in the Ne, Na, Mg, Al, P, Si, S group and 5 in the A, K, Ca group. No events were obtained for the Fe, Co, Ni group. Considering the limited statistics available and the altitude of the flight at this magnetic latitude, the results appear reasonable.

Additional data from flights conducted in July and August 1960 have only recently been obtained and have not yet been reduced.

The gold-silicon semiconductor detectors were developed too late in the program to be used in the balloon flight measurements. As an alternative, permission was requested and received to fly units in the Atlas-Able-5B and Ranger vehicles for evaluation in the space environment. To date, no data are available from tests conducted in flight.

Laboratory tests indicate that the detector elements may be fabricated in a manner which ensures long-term operation in a high or low temperature vacuum environment.

It is presently planned to use the equipment developed in breadboard under Contract No. NASw-24 in vehicles such as the Mariner series, in which data-handling and weight capabilities are sufficient to accommodate the instrumentation. The designs are being modified to include silicon circuit elements and, where possible, the AuSi detector, to lessen the weight, conserve space, and allow operation under more strenuous environments.

5. SUMMARY

Contract No. NASw-24 has provided a means for a number of developments for use in future spacecraft. These developments include:

1. Demonstration of the feasibility of a system for the determination

Table 3. Assignment of Values for Events from Data of the Balloon Flight Test on 19 August 1959

Event No.	Particle	Energy	Event No.	Particle	Energy
116	A^{40}, Ca^{40}	10^{14} ev/nucleon	62	Be^9	> 10 Bev/nucleon
111	C^{12}, N^{14}	$\begin{cases} C^{12} = 300 \text{ Mev/nucleon} \\ N^{14} = 250 \text{ Mev/nucleon} \end{cases}$	56	Be^9	40 Mev/nucleon
96	Si^{28}, S^{32}	~ 2 Bev/nucleon	55	A^{40}, K^{39}, Ca^{40}	> 10 Bev/nucleon
87	C^{12}	~ 2 Bev/nucleon	54	N^{14}	350 Mev/nucleon
85	A^{40}	~ 2 Bev/nucleon	48	Be^9	> 10 Bev/nucleon
80	Al^{27}	~ 2 Bev/nucleon	45	Li^7	~ 30 Mev/nucleon
79	Li^7	~ 60 Mev/nucleon	40	N^{14}, O^{16}	> 10^{14} ev/nucleon
77	B^{11}	2 Bev/nucleon	36	P^{31}	~ 160 Mev/nucleon
76	Li^7	50 Mev/nucleon	35	Si^{28}	90 Mev/nucleon
74	B^{11}	2 Bev/nucleon	26	F^{19}	350 Mev/nucleon
73	Li^7	50 Mev/nucleon	19	Ca^{40}, K^{39}, A^{40}	> 600 Mev/nucleon
69	Si^{28}	2 Bev/nucleon	18	O^{16}	400 Mev/nucleon
68	C, N, O	2 Bev/nucleon	10	N^{14}	400 Mev/nucleon
63	Be^9	50 Mev/nucleon	6	Ca^{40}, K^{39}, A^{40}	> 10 Bev/nucleon

of atomic number and energy of heavy cosmic-ray primaries.

2. Demonstration of a system for two-dimensional pulse-height analysis.

3. Development of a semiconductor detector device whose potential uses include proton range telescopes, direct measurement of dE/dx and E for the heavy primary component, and as a photodiode for scintillometry.

4. Development of instrumentation for measurement of the low-energy proton flux in the energy range 0.5 Mev and upward to the exclusion of background flux containing γ rays and electrons.

5. Exploration of packaging techniques which have led to significant reduction in space and weight requirements for electronic systems.